Cultural landscape: Towards the design of a nocturnal lightscape

engineering proceedings

Proceeding Paper

A Generalized Model to Describe Electromagnetic Shock Absorbers †

Gennaro Sorrentino [1,2,*], Renato Galluzzi [3,*], Andrea Tonoli [1,2] and Nicola Amati [1,2]

[1] Department of Mechanical and Aerospace Engineering, Politecnico di Torino, 10129 Turin, Italy; andrea.tonoli@polito.it (A.T.); nicola.amati@polito.it (N.A.)
[2] Center of Automotive Research and Sustainable Mobility, Politecnico di Torino, 10129 Turin, Italy
[3] School of Engineering and Sciences, Tecnologico de Monterrey, Mexico City 14380, Mexico
* Correspondence: gennaro.sorrentino@polito.it (G.S.); renato.galluzzi@tec.mx (R.G.)
† Presented at the 53rd Conference of the Italian Scientific Society of Mechanical Engineering Design (AIAS 2024), Naples, Italy, 4–7 September 2024.

Abstract: The development of chassis technologies has pushed significant focus towards electrification for enhanced vehicle efficiency, flexibility, safety, and performance. In this context, the suspension represents a key system, as it strongly influences both vehicle dynamics and comfort. The trend is to replace the usual hydraulic damper with mechatronic actuators. Rotary electromagnetic shock absorbers are among these solutions, featuring a rotary electric machine and a proper rotary-to-linear transmission stage. Far from being ideal force sources, these actuators may introduce inertial, compliance, and friction phenomena to the suspension. This paper proposes a generalized equivalent model to reproduce the mechanical behavior of electromagnetic shock absorbers. The formulation of this tool helps compare different shock absorber technologies in terms of their dynamic response. Furthermore, it can be used to synthesize control strategies that account for intrinsic limitations of chassis actuators.

Keywords: electromagnetic; shock absorber; actuator; active suspension; dynamic model

Academic Editors: Umberto Galietti, Gabriele Arcidiacono, Enrico Armentani, Davide Castagnetti, Vigilio Fontanari, Aurelio Somà and Nicola Bonora

Published: 14 February 2025

Citation: Sorrentino, G.; Galluzzi, R.; Tonoli, A.; Amati, N. A Generalized Model to Describe Electromagnetic Shock Absorbers. *Eng. Proc.* **2025**, *85*, 11. https://doi.org/10.3390/engproc2025085011

1. Introduction

Research and development in the automotive field are increasingly devoting their efforts into vehicle electrification to provide enhanced solutions among different subsystems. While full powertrain electrification represents the paramount of electrification, the adoption of mechatronic actuators for chassis functionalities embodies a natural evolution of automotive technologies. Electrified chassis components can synergistically contribute to the overall vehicle efficiency and enhancement of its performance, safety, and adaptability to the driver's feeling [1]. In this scenario, electrified controllable suspensions represent a key subsystem because they strongly influence both ride comfort and road holding.

Although semi-active suspensions have a significant presence in the market, the interest in full-active solutions has constantly increased in the last decade [2] thanks to a broader control freedom with respect to the semi-active ones. Indeed, full-active suspensions are force-controlled, while semi-active suspensions are damping-controlled; i.e., they are bounded by a passivity constraint. However, in the case of full-active suspensions, power consumption is the main drawback to be faced.

Electromagnetic shock absorbers feature an electric machine coupled to a transmission stage interfaced to the suspension assembly. They can provide forces in four quadrants: active and passive forces in both extension and compression phases. This translates into

motoring or braking behavior of the electric machine, which can absorb or exert power in the suspension thanks to its intrinsic reversibility. In the case of a controlled braking, the absorbed power can be partially harvested [3]. All in all, when compared to other active shock absorbers, electromagnetic dampers can show an improved efficiency and a lower average power consumption [4]. The natural stroke of the automotive suspensions may suggest the use of linear motors to accomplish active damping tasks. This is observed in early proposals of this technology [5,6]. However, linear machines exhibit a low force density, which usually leads to heavy and bulky actuators. Therefore, rotary electric machines stand out as a more favorable alternative, despite the need of a rotary-to-linear conversion stage. Usually, the latter is either hydraulic (e.g., by means of a cylinder coupled to a pump [7]) or mechanical (e.g., through ball-screws [8] or levers [9,10]).

Nevertheless, problems related to inertia, friction, and compliance arise with these more complex rotary systems. When introduced in the suspension, these actuators cannot be represented as ideal force sources. The aforementioned loss and dynamic contributions change the magnitude and phase of the actuator output. As such, the consideration of these effects is of fundamental importance. Li et al. [11] studied the effect of shock absorber non-idealities by modeling each subsystem of the actuator. Although the model closely reproduces the experimental results, it appears very complex to be experimentally identified and managed for control synthesis. Instead, Kawamoto et al. [12] embodied the electromagnetic damper non-idealities in a quarter car model to test its active functionality. However, the use of a mass that lumps the inertial properties of the actuator misleads its real working principle. Indeed, these contributions must be lumped as an inertance term that reacts to the relative acceleration of the suspension.

By generalizing the dynamic model studied by Tonoli et al. [13], the contribution of this paper is to propose a generalized equivalent representation of the electromagnetic shock absorber in the linear mechanical domain. This tool presents three key features: (i) it can be used to describe the dynamic behavior of any electromagnetic shock absorber technology, (ii) its analysis can help to establish a quantitative comparison among diverse technologies thanks to the presence of fewer parameters to be identified, and (iii) it can be used in the synthesis of control techniques by introducing the relative suspension speed as input.

This paper is organized as follows: Section 2 presents the proposed model applied to two case studies, including both a full and a simplified version of the model. Then, Section 3 shows numerical results from the two case studies. A benchmark of the two case studies is performed by comparing their respective model features. Finally, Section 4 concludes this manuscript.

2. Materials and Methods

In this section, two technologies of electromagnetic shock absorber under study are first described. Then, a generalized model is proposed to describe the mechanical dynamic behavior of the aforementioned actuators. Finally, the model is simplified into a single-input, single-output system.

2.1. Electro-Hydrostatic Shock Absorber

The proposed electromagnetic shock absorber is based on the prototype presented by Puliti et al. [14]. As depicted in Figure 1, a rotary electric machine is coupled to a gerotor pump and together they supply a controlled differential pressure to a monotube damper.

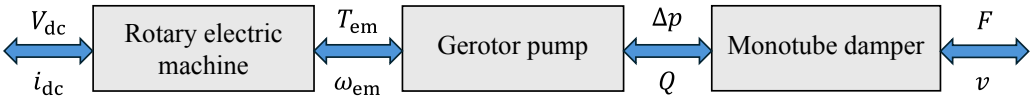

Figure 1. Working principle of an electro-hydrostatic shock absorber.

Specifically, the electric motor is a three-phase surface-mounted permanent-magnet synchronous motor; its shaft is rigidly connected to the inner gear of the pump. The relative rotation of the inner gear with respect to the outer gear produces a volume variation in the pump chambers created in between the teeth, resulting in an increase in hydraulic pressure. The pump feeds directly the lower chamber of the damper, while the upper one is kept with a constant preload by means of an accumulator. Hence, the differential pressure Δp can be both positive or negative, turning, respectively, into an extension or compression force F thanks to the damper piston. This force acts directly on the suspension mounts. For the sake of simplicity, this solution will be referred to as the electro-hystrostatic actuator (EHA).

Figure 2 shows the case study prototype, with a focus on its motor-pump unit. The main advantages of this solution are the straightforward implementation into the suspension architecture, the reliability against fatigue and wear due to the intrinsic lubrication, and the fail-safe damping thanks to its viscous damping response and its hydraulic leakages [15]. Fail-safe damping is required in case of any electrical fault; hence, it should appear without any contribution of the electric machine (open-circuit damping). However, its presence results in a reduced total conversion efficiency, with peak values around 50% [14]. Another drawback is its large inertia seen by the suspension. This effect can be attributed to all the rotating elements inside the motor-pump unit.

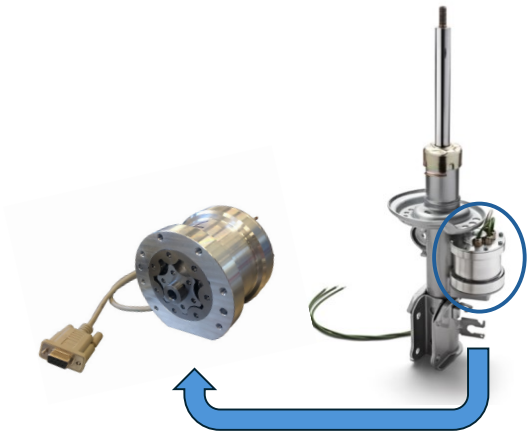

Figure 2. Electro-hydrostatic shock absorber prototype.

2.2. Electro-Mechanical Shock Absorber

The second electromagnetic shock absorber solution under study is a full electro-mechanical one. The first iteration of this kind of active shock absorber was disseminated by Galluzzi et al. [16]. Similarly to the EHA, its working principle is depicted in Figure 3.

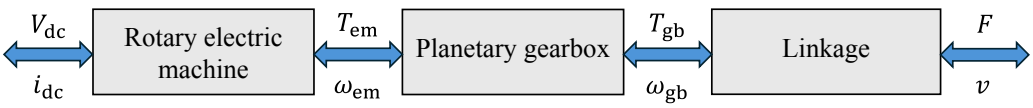

Figure 3. Working principle of an electro-mechanical shock absorber.

In particular, the pump is replaced by an oil-free planetary gearbox. The latter is a two-stage speed multiplier where the sun of the first stage is machined into the electric machine shaft and the outer shaft is the carrier of the second stage. In this case, both stages

have the same transmission ratio. The rotary-to-linear conversion happens by means of a linkage mechanism; a rocker arm is connected to the outer shaft through a splined profile and its free end is connected to a linking rod with a ball joint. Eventually, the rod is coupled to the suspension, so the linear passive damper can be removed. For the sake of simplicity, this solution will be referred as rotary (ROT).

The ROT prototype is shown in Figure 4. Its main strength is the higher conversion efficiency when compared to the EHA, with a peak around 80% [16]. This behavior derives from lower friction, but the open-circuit damping alone is not sufficient to guarantee fail-safe operation. The overall inertia decreases because the pitch diameter of the high-speed sun is comparable to that of the motor shaft. All the other rotating elements contribute less impact due to the several intermediate transmission ratios. Nevertheless, the presence of many spinning gears drastically increases acoustic emissions, giving rise to new challenges for suspension noise, vibration, and harshness. The suspension packaging is a very important challenge too, because it requires structural modifications to accommodate the electric drive and its lever system.

Figure 4. Electro-mechanical shock absorber prototype.

2.3. Generalized Model

From previous sections, an optimal full-active solution is difficult to identify. Despite this, a generalized equivalent model could help in understanding and comparing the dynamic performance of different electromagnetic shock absorbers at the suspension level. It is also useful for enhancing the linear suspension models for control studies.

The proposed general model in Figure 5 is an equivalent linear mechanical model of the active damper. It lumps its dissipative, elastic, and inertial properties. In particular, the equivalent viscous damping c_{eq} groups the internal friction due to the moving parts. The equivalent mass m_{eq} accounts for inertial effects. The damping c_l represents the leakages in the hydraulic circuit; thus, it is infinitely large for fully mechanical solutions. Moreover, a spring–damper parallel lumps the compliance of the force–motion transmission to the suspension. These systems are usually characterized by a series of stiffness contributions—mechanical or hydraulic—where the less stiff component dominates the coefficient k_m. Compliant behavior is accompanied by a slight viscous loss lumped in c_m. An ideal force actuator applies the desired force F_a to the system, reproducing the action of the controlled electric machine. Indeed, in a purely passive setup, the motor can be shunted with an external active load R_{ext}. In this way, the ideal force actuator is replaced by an RL series load constituted by resistance $R + R_{ext}$ and inductance L [13]. Here, R and L are the electric machine winding resistance and inductance of the electric machine, respectively. However, if the machine is current-controlled at a sufficiently large bandwidth (above 1 kHz), the ideal force actuator representation holds validity. In the end, the model is balanced by the suspension force F applied to its free end, which represents the suspension top mount.

Although this model is consistent with the behavior of linear dampers, rotary technologies require the definition of a rotary-to-linear transmission ratio:

$$\tau_\ell = \frac{v}{\omega_{\text{out}}} \tag{1}$$

where v is the suspension linear relative speed and ω_{out} is the output shaft angular speed. Thus, all the rotary parameters can be linearized as follows:

$$m_{\text{eq}} = \frac{J_{\text{out}}}{\tau_\ell^2} \tag{2}$$

$$c_{\text{eq}} = \frac{\Gamma_{\text{out}}}{\tau_\ell^2} \tag{3}$$

where J_{out} combines all the rotating inertias at the output shaft and Γ_{out} all the friction terms. For the EHA, ω_{out} coincides with the electric machine speed ω_{em}, whereas for the ROT, it coincides with the output shaft speed, i.e., downstream the gearbox. However, for the EHA, the piston mass and frictions must be added, too. Although this representation is being introduced for electromagnetic shock absorbers, it can be applied to a wide range of force or servo actuators where linear-to-rotary conversion is exploited. Actuators employed in aerospace applications could be represented through a similar model [15].

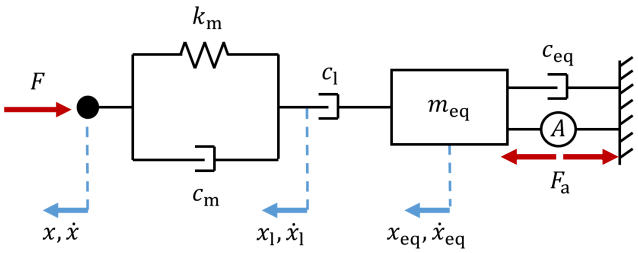

Figure 5. Equivalent linear mechanical model of an electromagnetic shock absorber.

The equations of motion of the model can be obtained applying the Lagrange's equation:

$$\frac{d}{dt}\left(\frac{\partial \mathcal{L}}{\partial \dot{q}}\right) - \frac{\partial \mathcal{L}}{\partial q} + \frac{\partial \mathcal{F}}{\partial \dot{q}} = \frac{\partial \delta W}{\partial \delta q} \tag{4}$$

where the Lagrangian term $\mathcal{L}$ is the difference between the kinetic energy of the system $\mathcal{T}$ and the potential energy $\mathcal{U}$, $\mathcal{F}$ is the dissipated energy, and δW is the virtual work. For this model, the degrees of freedom are $q = \{x, x_{\text{l}}, x_{\text{eq}}\}^\intercal$ and the following expressions are valid:

$$\mathcal{T} = \frac{1}{2} m_{\text{eq}} \dot{x}_{\text{eq}}^2 \tag{5}$$

$$\mathcal{U} = \frac{1}{2} k_{\text{m}} (x - x_{\text{l}})^2 \tag{6}$$

$$\mathcal{F} = \frac{1}{2} c_{\text{eq}} \dot{x}_{\text{eq}}^2 + \frac{1}{2} c_{\text{l}} (\dot{x}_{\text{l}} - \dot{x}_{\text{eq}})^2 + \frac{1}{2} c_{\text{m}} (\dot{x} - \dot{x}_{\text{l}})^2 \tag{7}$$

$$\delta W = F_{\text{a}} \delta x_{\text{eq}} - F \delta x \tag{8}$$

In the end, the following system of equations governs the model dynamics:

$$\begin{cases} k_{\text{m}}(x - x_{\text{l}}) + c_{\text{m}}(\dot{x} - \dot{x}_{\text{l}}) = -F \\ k_{\text{m}}(x - x_{\text{l}}) + c_{\text{m}}(\dot{x} - \dot{x}_{\text{l}}) = c_{\text{l}}(\dot{x}_{\text{l}} - \dot{x}_{\text{eq}}) \\ m_{\text{eq}} \ddot{x}_{\text{eq}} + c_{\text{eq}} \dot{x}_{\text{eq}} - c_{\text{l}}(\dot{x}_{\text{l}} - \dot{x}_{\text{eq}}) = F_{\text{a}} \end{cases} \tag{9}$$

Combining the equations in (9) in the Laplace domain, the model can be expressed by a multiple-input, single-output (MISO) expression. The output is the force exerted on the suspension $F(s)$, and the two inputs are the speed of the free end $v(s) = sx(s)$ and the actuation force $F_a(s)$:

$$F(s) = \underbrace{\frac{c_l(k_m + sc_m)}{D(s)}}_{H_a(s)} F_a(s) \underbrace{- \frac{c_l(k_m + sc_m)(sm_{eq} + c_{eq})}{D(s)}}_{H_v(s)} v(s) \tag{10}$$

where

$$D(s) = c_l(k_m + sc_m) + (sm_{eq} + c_{eq})[k_m + s(c_m + c_l)] \tag{11}$$

The transfer function $H_a(s)$ links the actuation force with the output and it is a mechanical filter. The transfer function $H_v(s)$ links the free-end speed with the output and it is a dynamic mechanical impedance. Overall, the two contributions are combined linearly to determine the output force F in frequency domain.

2.4. Simplified Model

The actuation force F_a can be determined by a suspension-level control strategy. Although multiple control laws can be applied for different purposes, a simple strategy is to reproduce the behavior of an ideal viscous damper, i.e., $F_a = -c_a v$. In certain instances, this allows for energy regeneration. From a mathematical standpoint, this choice simplifies (10) by dividing both sides by the free-end speed v. The result is a single-input, single-output (SISO) mechanical impedance:

$$c_t(s) = -\frac{F(s)}{v(s)} = \frac{(k_m + sc_m)(sm_{eq} + c_{eq} + c_a)}{(k_m + sc_m) + (sm_{eq} + c_{eq})[k_m/c_l + s(c_m/c_l + 1)]} \tag{12}$$

It is characterized by a second-order mechanical filter multiplying a damping term, which is sum of the controlled damping c_a and the dynamic mechanical damping of the system $sm_{eq} + c_{eq}$. For full electro-mechanical shock absorbers as the ROT, (12) can be further simplified because the leakage term obeys $c_l \to \infty$. Hence,

$$\lim_{c_l \to \infty} c_t(s) = \frac{(k_m + sc_m)(sm_{eq} + c_{eq} + c_a)}{m_{eq}s^2 + (c_{eq} + c_m)s + k_m} \tag{13}$$

From (13), the second-order filtering behavior is much clearer.

3. Results

This section presents numerical results of the models described in Section 2. The case studies are the technologies also presented in Section 2; Table 1 reports their lumped parameters computed through experimental campaigns in previous works [14,16].

Table 1. Lumped parameters of the EHA and ROT.

Description	Symbol	Value		Unit
		EHA	ROT	
Equivalent damping due to friction	c_{eq}	1000	250	Ns/m
Equivalent mass	m_{eq}	100	5.6	kg
Leakage damping	c_l	$1.7 \cdot 10^4$	∞	Ns/m
Transmission compliance damping	c_m	50	50	Ns/m
Transmission compliance stiffness	k_m	$3.2 \cdot 10^4$	$2 \cdot 10^5$	N/m

3.1. Generalized Model

The generalized MISO model can be divided into the sum of two contributions, as already stated in Section 2.3. Considering $s = j\omega$, the transfer function of the output force from the actuation force H_a can be plotted in the frequency domain (Figure 6). The two technologies are compared in this graph. Both prototypes show a unitary gain at low frequency and a null phase lag, meaning that the output force F is exactly in phase and equal in magnitude to the actuation force F_a. More accurately, the EHA static gain is 0.95 because an increased leakage flow yields a lower damping c_l, which hinders the effectiveness of the force transmission. Two resonant peaks arise, respectively, at 2.6 Hz for the EHA and 30 Hz for the ROT. This translates into a wider actuation bandwidth for the ROT prototype of almost a decade. However, the increased losses in the EHA attenuates more effectively the resonant peak, limiting the unwanted magnitude amplification. This phenomenon denotes the interaction between inertial (m_{eq}) and stiffness (k_m) terms. Afterwards, both systems are dominated by their compliance. In particular, the EHA has a stiffness k_m one order of magnitude lower than the ROT. In the former case, transmission stiffness is dominated by the oil bulk modulus. In the latter, the gear tooth stiffness plays a fundamental role.

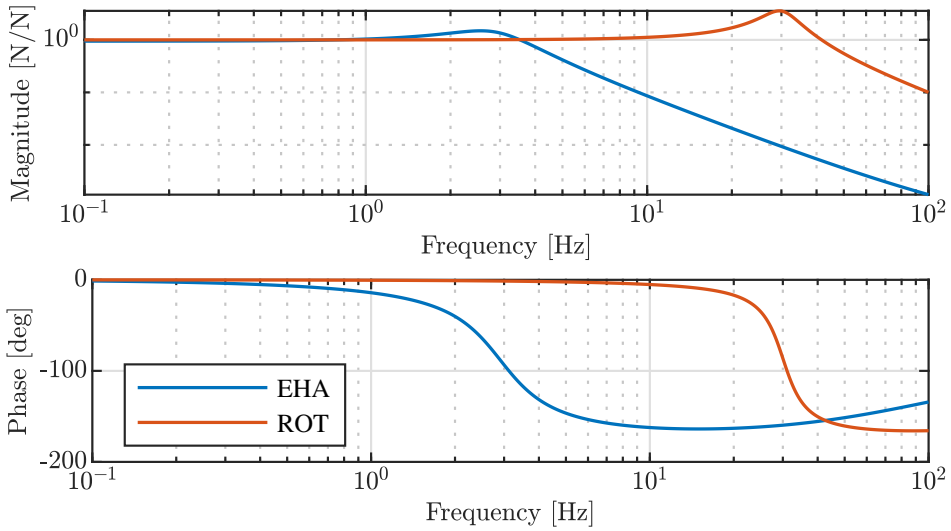

Figure 6. MISO model: actuation force to output force transfer function $H_a(s)$ in the frequency domain. Magnitude (**top**) and phase (**bottom**) responses.

The transfer function described by the output force over the free-end speed ($H_v(s)$) is shown in Figure 7. At low frequency, this dynamic damping is governed by the internal friction lumped in c_{eq} and the output force F is in phase opposition with respect to the speed v. Also, in this case, the presence of leakages lowers the static gain of the EHA impedance with respect to c_{eq}. As the resonant frequencies are approached, the systems tend to act as an inerter. This is confirmed by the increase in mechanical impedance (self-locking effect) and the phase growth towards -90 deg. Heavy attenuation comes after the resonant peak, where the transmission compliance given by k_m dominates.

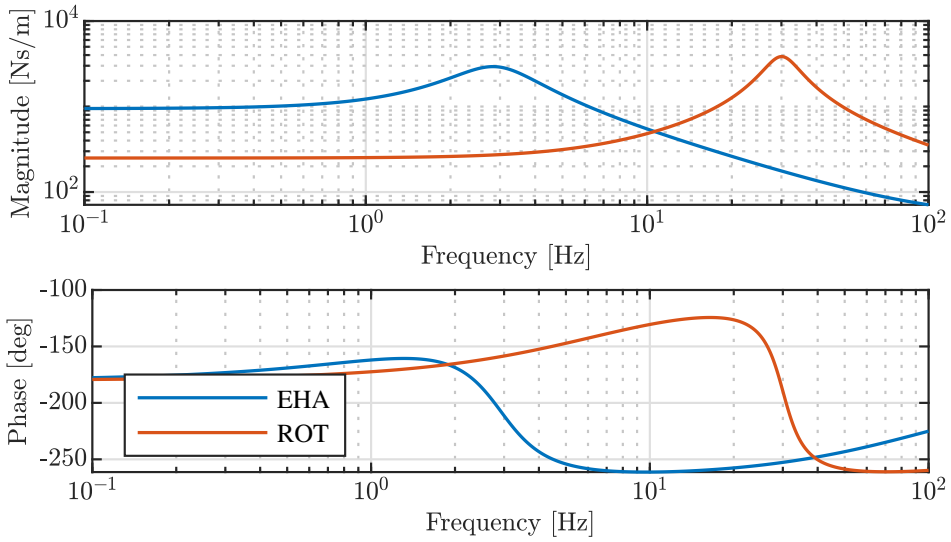

Figure 7. MISO model: free-end speed to output force transfer function $H_{\mathrm{v}}(s)$ in the frequency domain. Magnitude (**top**) and phase (**bottom**) responses.

3.2. Simplified Model

The simplified SISO model reduces to a mechanical impedance transfer function. The two case studies are shown in Figure 8 for the EHA and in Figure 9 for the ROT. The actuation damping c_{a} is parameterized from 0 to 3 kNs/m. The shape follows the transfer function $H_{\mathrm{v}}(s)$ both in module and phase. In fact, the static gain is still the value of damping c_{eq}, slightly affected by the leakages in c_{l}, where present. In both prototypes, the action of the actuation damping c_{a} increases the gain at low frequencies, and limits the resonant amplification and the inerter effect.

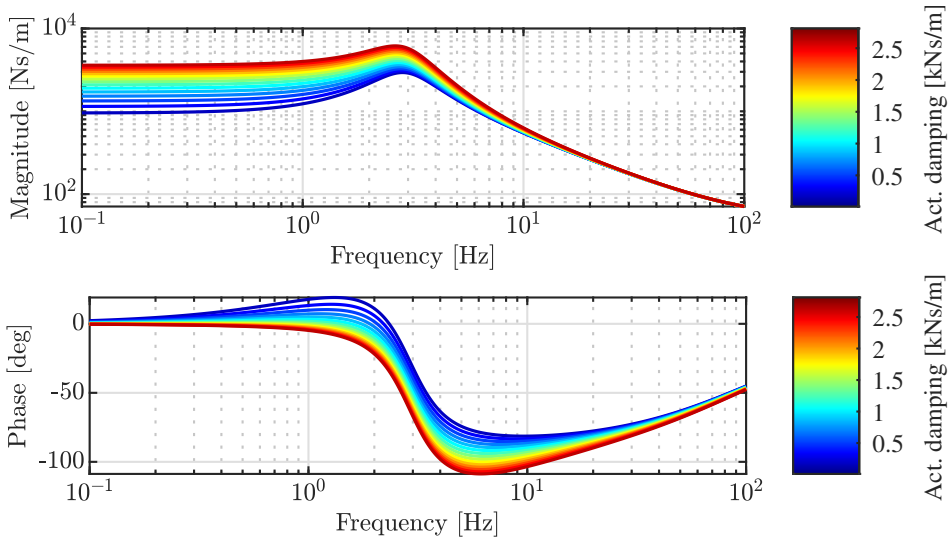

Figure 8. SISO model: mechanical impedance $c_{\mathrm{t}}(s)$ of the EHA prototype varying the actuation damping c_{a}. Magnitude (**top**) and phase (**bottom**) responses.

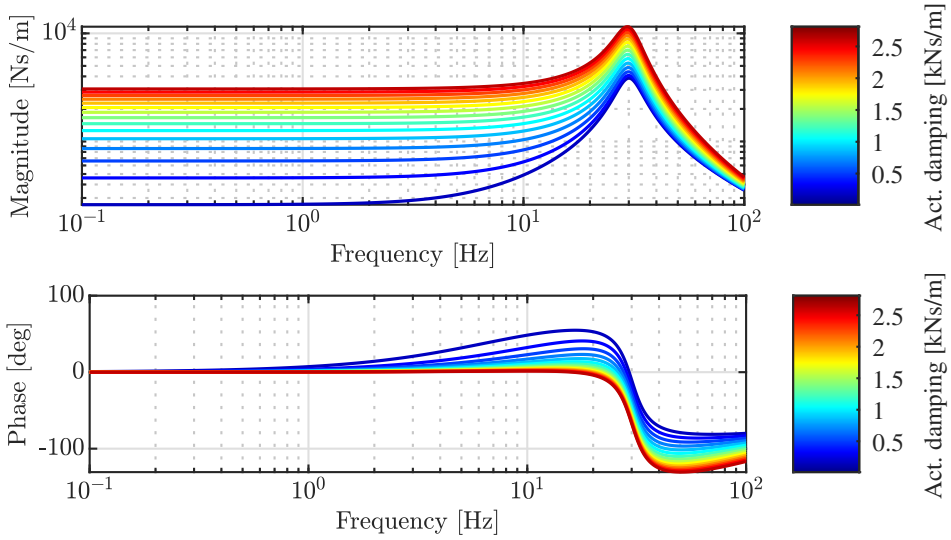

Figure 9. SISO model: mechanical impedance $c_t(s)$ of the ROT prototype varying the actuation damping c_a. Magnitude (**top**) and phase (**bottom**) responses.

3.3. Discussion

The resulting dynamic features of both the EHA and ROT are summarized in Table 2. Both models—generalized and simplified—highlight the wide actuation bandwidth offered by the ROT device. This feature are applicable to most electro-mechanical shock absorbers in the literature. This allows classifying the ROT device as a full-active system covering both sprung mass natural frequency (∼1–1.5 Hz) and unsprung mass natural frequency (∼10–15 Hz). The latter is of extreme importance when road holding control strategies are pursued. However, its tendency to act as an inerter at high frequency must be taken into account, as it might provide unwanted out-of-phase forces into the suspension that can make the vehicle unstable. The limited internal friction lumped in c_{eq} justify the higher conversion efficiency and the low open-circuit damping, as also shown in Figure 7.

Despite its more limited bandwidth, the EHA can still cover the sprung mass natural frequency and it can control the comfort frequency range (from 4 to 8 Hz) well enough, especially if a force feedback control is implemented. The EHA can also fully control body motion during handling maneuvers involving pitch and roll. The more relevant frictions and the leakage contributions explain the lower conversion efficiency and the higher open-circuit damping. This latter term is a desirable feature that guarantees a safe vehicle maneuverability in case of any electric failure.

Table 2. Main dynamic features of the EHA and ROT.

Description	Value		Unit
	EHA	ROT	
Resonant peak frequency	2.6	30	Hz
Output force static gain	0.95	1	N/N
Output force resonant gain	1.5	3.6	N/N
Static mechanical impedance gain	948	250	Ns/m
Resonant mechanical impedance gain	2931	3837	Ns/m
Phase lag at resonance	−161	−124	deg

4. Conclusions

The present paper provides a generalized tool to analyze the dynamic behavior of electromagnetic shock absorbers. An equivalent linear mechanical model is proposed to fit both linear and rotary solutions of hydraulic or mechanical nature. Regardless,

any rotary damper requires a rotary-to-linear transmission. It is a simple single mass model merging the inertial, compliant, and dissipative features of the actuator in lumped parameters. Moreover, it takes into account the relative motion affecting the shock absorber by assuming the suspension relative speed as an input at the actuator free end. Once the damper model is derived, it can be expressed by a MISO formulation, where the input are the actuation force developed by the electric machine and the suspension speed. Alternatively, it can be further simplified to a SISO system considering a damping control strategy for the actuation.

The case study results show a wider bandwidth for the electro-mechanical shock absorber (ROT) but a strong influence of its inertia at higher frequency. On the other hand, the electro-hydraulic shock absorber (EHA) can cover a lower-frequency output force, but it still guarantees actuation bandwidth for sprung mass control and comfort. Furthermore, leakages and internal frictions damp the inertia influence on the dynamic response and guarantee fail-safe operation.

This shock absorber model can be useful for updating vehicle dynamics models (quarter-, half-, or full-car models) with a realistic active damper. Model-based control strategies would gain a more accurate representation of the actuator dynamics for a more accurate control synthesis.

Author Contributions: Conceptualization, G.S., R.G., A.T. and N.A.; methodology, G.S., R.G., A.T. and N.A.; formal analysis, G.S. and R.G.; investigation, G.S. and R.G.; writing—original draft preparation, G.S.; writing—review and editing, G.S. and R.G.; supervision, A.T. and N.A. All authors have read and agreed to the published version of the manuscript.

Funding: The activity has been partially financed by the European Union—Next Generation EU—PNRR M4C2, Investimento 1.4—Avviso n. 3138 del 16/12/2021—CN00000023 Sustainable Mobility Center (Centro Nazionale per la Mobilita' Sostenibile)—CNMS—CUP E13C22000980001. This publication is also part of the project NODES which has received funding from the MUR—M4C2 1.5 of PNRR with grant agreement no. ECS00000036.

Data Availability Statement: No new data were created or analyzed in this study. Data sharing is not applicable to this article.

Acknowledgments: The authors would like to thank the staff at Marelli Ride Dynamics for their valuable support throughout this research activity.

Conflicts of Interest: The authors declare no conflicts of interest.

Abbreviations

The following abbreviations are used in this manuscript:

EHA	Electro-Hydrostatically Actuated Shock Absorber
ROT	Rotary Electro-mechanical Shock Absorber
MISO	Multi Input Single Output
SISO	Single Input Single Output

References

1. Mazzilli, V.; De Pinto, S.; Pascali, L.; Contrino, M.; Bottiglione, F.; Mantriota, G.; Gruber, P.; Sorniotti, A. Integrated chassis control: Classification, analysis and future trends. *Annu. Rev. Control* **2021**, *51*, 172–205. [CrossRef]
2. Yu, M.; Evangelou, S.A.; Dini, D. Advances in Active Suspension Systems for Road Vehicles. *Engineering* **2024**, *33*, 160–177. [CrossRef]
3. Zuo, L.; Zhang, P.S. Energy harvesting, ride comfort, and road handling of regenerative vehicle suspensions. *J. Vib. Acoust.* **2013**, *135*, 011002. [CrossRef]
4. Abdelkareem, M.A.; Xu, L.; Ali, M.K.A.; Elagouz, A.; Mi, J.; Guo, S.; Liu, Y.; Zuo, L. Vibration energy harvesting in automotive suspension system: A detailed review. *Appl. Energy* **2018**, *229*, 672–699. [CrossRef]

5. Karnopp, D. Permanent magnet linear motors used as variable mechanical dampers for vehicle suspensions. *Veh. Syst. Dyn.* **1989**, *18*, 187–200. [CrossRef]
6. Klimenko, Y.I.; Batishchev, D.; Pavlenko, A.; Grinchenkov, V. Design of a linear electromechanical actuator with an active vehicle suspension system. *Russ. Electr. Eng.* **2015**, *86*, 588–593. [CrossRef]
7. Fang, Z.; Guo, X.; Xu, L.; Zhang, H. Experimental study of damping and energy regeneration characteristics of a hydraulic electromagnetic shock absorber. *Adv. Mech. Eng.* **2013**, *5*, 943528. [CrossRef]
8. Liu, Y.; Xu, L.; Zuo, L. Design, modeling, lab, and field tests of a mechanical-motion-rectifier-based energy harvester using a ball-screw mechanism. *IEEE/ASME Trans. Mechatron.* **2017**, *22*, 1933–1943. [CrossRef]
9. Arana, C.; Evangelou, S.A.; Dini, D. Series active variable geometry suspension for road vehicles. *IEEE/ASME Trans. Mechatron.* **2014**, *20*, 361–372. [CrossRef]
10. Yu, M.; Arana, C.; Evangelou, S.A.; Dini, D.; Cleaver, G.D. Parallel active link suspension: A quarter-car experimental study. *IEEE/ASME Trans. Mechatron.* **2018**, *23*, 2066–2077. [CrossRef]
11. Li, Z.; Brindak, Z.; Zuo, L. Modeling of an electromagnetic vibration energy harvester with motion magnification. In Proceedings of the ASME International Mechanical Engineering Congress and Exposition, Denver, CO, USA, 11–17 November 2011; Volume 54938, pp. 285–293.
12. Kawamoto, Y.; Suda, Y.; Inoue, H.; Kondo, T. Modeling of electromagnetic damper for automobile suspension. *J. Syst. Des. Dyn.* **2007**, *1*, 524–535. [CrossRef]
13. Tonoli, A.; Amati, N.; Detoni, J.G.; Galluzzi, R.; Gasparin, E. Modelling and validation of electromechanical shock absorbers. *Veh. Syst. Dyn.* **2013**, *51*, 1186–1199. [CrossRef]
14. Puliti, M.; Galluzzi, R.; Tessari, F.; Amati, N.; Tonoli, A. Energy efficient design of regenerative shock absorbers for automotive suspensions: A multi-objective optimization framework. *Appl. Energy* **2024**, *358*, 122542. [CrossRef]
15. Galluzzi, R.; Tonoli, A.; Amati, N. Modeling, control, and validation of electrohydrostatic shock absorbers. *J. Vib. Acoust.* **2015**, *137*, 011012. [CrossRef]
16. Galluzzi, R.; Circosta, S.; Amati, N.; Tonoli, A. Rotary regenerative shock absorbers for automotive suspensions. *Mechatronics* **2021**, *77*, 102580. [CrossRef]